World Academy of Science, Engineering and Technology
International Journal of Mechanical and Mechatronics Engineering
Vol:4, No:11, 2010

Three-dimensional Simulation of Flow Pattern at the Lateral Intake in Straight Path, using Finite-Volume Method

R.Goudarzizadeh, N.Hedayat and S.H.Mousavi Jahromi

Abstract**—**Channel junctions can be analyzed in two ways of division (lateral intake) and combined flows (confluence). The present paper investigates 3D flow pattern at lateral intake using Navier-Stokes equation and $\kappa-\varepsilon$ (RNG) turbulent model. The equations are solved by Finite-Volume Method (FVM) and results are compared with the experimental data of (Barkdoll, B.D., 1997) to test the validity of the findings. Comparison of the results with the experimental data indicated a close proximity between the two sets of data which suggest a very close simulation. Results further indicated an inverse relation between the effects of discharge ratio (Q_r) on the length and width of the separation zone. In other words, as the discharge ration increases, the length and width of separation zone decreases.

Keywords**—**90^0 junction, flow division, turbulent flow, numerical modeling, flow separation zone.

I. Introduction

RIVERS and streams are considered as natural flow of the surface run-offs which are either permanent or seasonal and in their flow path may have various junctions. These junctions appear either as division or confluence. The flow at the junction is usually very turbulent and has a complex and 3D state (Fig.1).

In this study investigates the flow pattern at the lateral intake structure in straight path because of its importance to meet the requirements of various demand sectors.

Various studies have been conducted in this respect. Taylor's experimental investigation of flow diversion in an open-channel whose conclusion was that the lose to the intake structure was shown to be approximately 2% of maximum water depth for a wide ranging Froude numbers and discharge ratios[12].

R.Goudarzizadeh, Post-graduate researcher, Islamic Azad University, Dezful Branch, Iran.
N.Hedayat, Dean, Faculty of Agriculture, Islamic Azad University, Dezful Branch, Iran.
S.H.Mousavi Jahromi, Associate professor, S.Chamran University, Ahwaz, Iran.

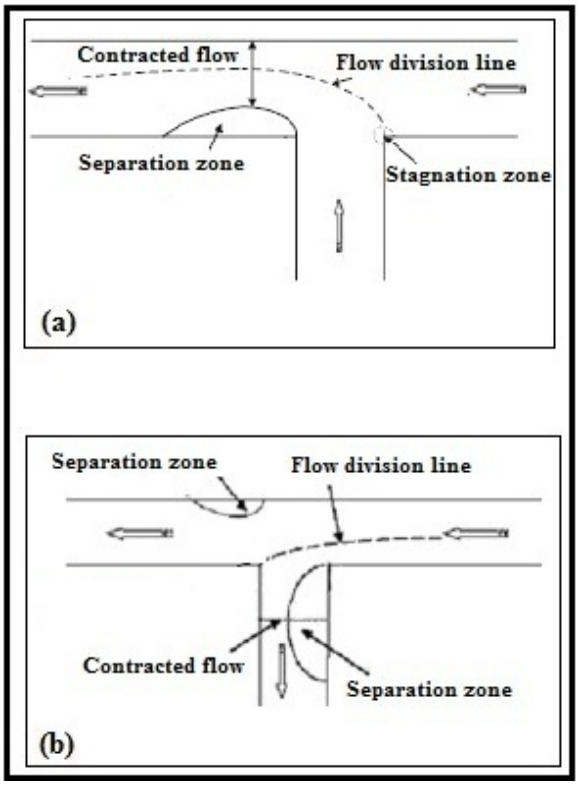

Fig. 1 Flow pattern at 90 degree T junctions in two state: (a) Confluence, (b) Lateral intake

[2] Experimented the flow division in a channel vis-a-vis various angles and presented their graphical findings in the form of dimensionless parameters.

[6] Have made experimental and analytical studies on main and side-channels having equal widths. They presented a relation for the discharge ratios for the Froude numbers before and after the junction as well as the ratio of width of the diversion channel to main-channel.

[5], [7], [11] Further indicated that under conditions where the Froude number is between 0.3 to 0.35 in 90 junction, the flow conditions at the intake reach will usually appear as non-submerged.

[1] Compared flow in an open-channel having 1 to 2 width to depth ratio with a flow pipe having 1 to 4 width to depth ratio. This researcher attributed the velocity difference in the

vicinity of water surface to secondary flow in the open-channel and its absence in the flow pipe.

The present paper is based on the experimental investigation model of [1] and the flow velocity is calculated by the $\kappa-\varepsilon$ (RNG) turbulent model. The findings are then compared with the experimental results at various cross-sections. The effects of discharge ratio on dimension of separation zone in channel junction are investigated to find out the ways in which it could influence the dimensions of the separation zone.

II. Materials And Methods

A. The Laboratory Model Specifications

The specifications of the laboratory used in this study are modeled on the channel structures that were originally developed and tested empirically by [1]. The main-channel was designed with a length of 2.74 m and the side-channel having a 1.68 m. The side-channel in this experiment was situated at 1 m downstream of the main-channel entrance. The width that was chosen for the two experimental channels was 0.152 m. The distinguishing feature of the experimental channel was in its design configuration that incorporate a horizontal bed at all locations as can be seen in figure 2.

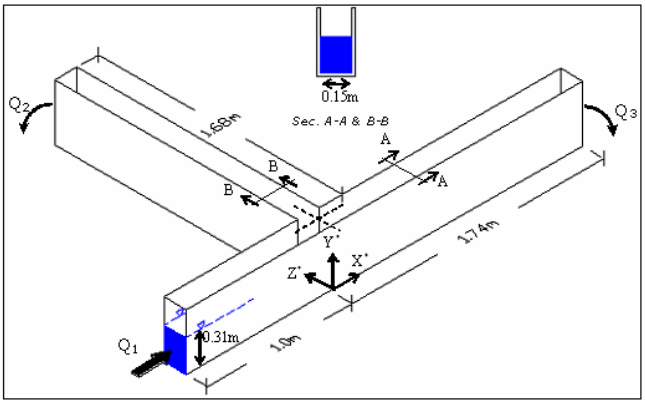

Fig. 2 The laboratory features of the experimental flume

The major experimental parameters consisted of a total discharge assumed at 0.011 m^3/sec and the depth H_0 fixed at 0.31 m. The average velocity in entrance channel was then assumed at u_0=0.234 m/sec. The Frude and Reynolds numbers were set at 0.13 and 72368 respectively. The details are shown in table 1.

TABLE I
HYDRAULIC CHARECTERISTICS OF THE COFLUENCE FLOW

Q (m^3/sec)	H_0 (m)	U_0 (m/sec)	Q_r	F_r	R_e
0.011	0.31	0.234	0.31	0.13	72368

B. Governing Equations

The equations used as the theoretical framework for the analysis of open-channel in this experiment consisted of Reynolds-Averaged Navier-Stokes (RANS) that governs the fluid dynamics that are assumed to have incompressible and steady state characteristics. The steady-state equations (mass continuity) and (momentum) are expressed as follows [10]:

- Continuity equation:

$$\frac{\partial u_i}{\partial x_i} = 0 \tag{1}$$

-Momentum equation:

$$\frac{\partial u_i}{\partial t} + \frac{\partial u_i u_j}{\partial x_j} = -\frac{1}{\rho}\frac{\partial P}{\partial x_i} + g_i + \frac{\partial}{\partial x_j}(\tau_{ij}) \tag{2}$$

This study also incorporated the Finite-Volume method as an analytical framework to discretize the equations.

C. Boundary Conditions

In the main-channel inlet, average velocity is adapted. Since the inlet velocity under the laboratory conditions is non-uniform in depth, the length of the main-channel should increase in order to establish the appropriate laboratory conditions.

An outflow boundary condition is adapted for the main and side-channel outlet. For using this boundary condition, the length of downstream main-channel and side-channel are adapted 2.5m.

The boundary conditions of the channel rigid zone are assumed to be wall and from the hydraulic point of view the surface of the channel walls are assumed to be smooth. The variations in water surface are ignored [12], the symmetry boundary conditions for the water surface were applied and the flow depth is H_0=0.31 which rendered it unnecessary to use the two-phased modeling that is costly. The grid independent test for the size is carried out which ultimately led to a choice of grid with 145×35×30 cells in the main-channel and 45×35×30 cells in the side-channel as is illustrated in figure 3.

The standard wall function is applied here in order to establish a relation between the sub-layer and the fully-turbulent layer.

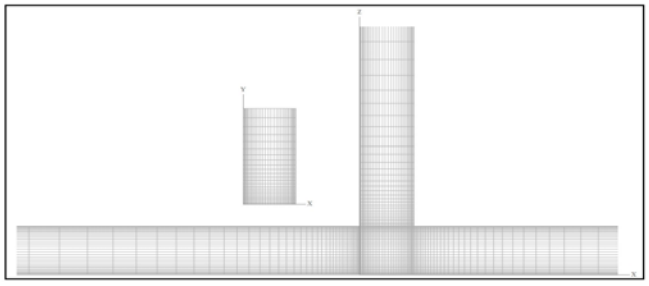

Fig. 3 Meshing system

D. Turbulent Model

[13] Presented a new version of the $k-\varepsilon$ turbulent model, the performance characteristics of which were optimized compared with the standard model. This model was based on the renormalization Group theory, the form of their equation is as follows:

$$\frac{\partial}{\partial t}(\rho\kappa)+\frac{\partial}{\partial x_i}(\rho\kappa u_i)=\frac{\partial}{\partial x_j}\left[\left(\mu+\frac{\mu_t}{\sigma_k}\right)\frac{\partial\kappa}{\partial x_j}\right]+P_\kappa-\rho\varepsilon \quad (3\text{-a})$$

$$\frac{\partial}{\partial t}(\rho\varepsilon)+\frac{\partial}{\partial x_i}(\rho\varepsilon u_i)=\frac{\partial}{\partial x_j}\left[\left(\mu+\frac{\mu_t}{\sigma_\varepsilon}\right)\frac{\partial\varepsilon}{\partial x_j}\right]+C_{1\varepsilon}\frac{\varepsilon}{\kappa}P_\kappa - \frac{C_u\eta^3\left(1-\frac{\eta}{\eta_0}\right)}{1+\beta\eta^3}\frac{\varepsilon^2}{\kappa} \quad (3\text{-b})$$

In equation (3-b), η is expressed as follow:

$$\eta=S\frac{\kappa}{\varepsilon}, S=\left(2S_{ij}S_{ij}\right)^{1/2}, S_{ij}=\frac{1}{2}\left(u_{i,j}+u_{j,i}\right) \quad (4)$$

TABLE II
EMPERICAL CONESTANT USED IN $k-\varepsilon$ (RNG) TURBULENT MODEL

β	η_0	σ_κ	σ_ε	C_u	$C_{1\varepsilon}$	$C_{2\varepsilon}$	k
0.012	4.38	0.7194	0.7194	0.0845	1.42	1.68	0.388

III. RESULTS AND DISCUSSIONS

Results show a close proximity between the estimated flow velocities at the main-channel length with the experimental data (Fig.4). They indicate that the velocity profile preserves and maintains its developed state ($X^*=-4.15$) at a distance before the intake structure. As water flow gets closer to the intake structure, the maximum velocity due to suction pressure is moved to the intake structure.

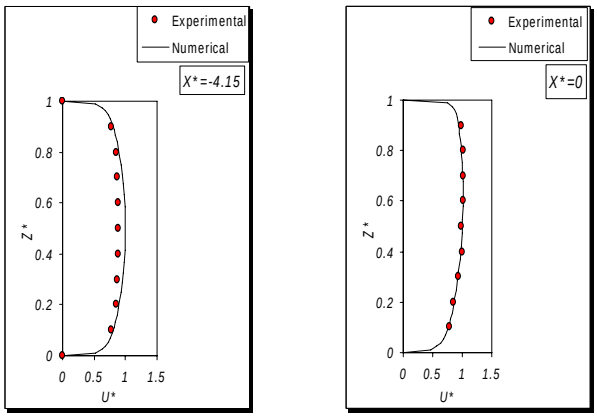

Fig. 4 Velocity profile along main-channel

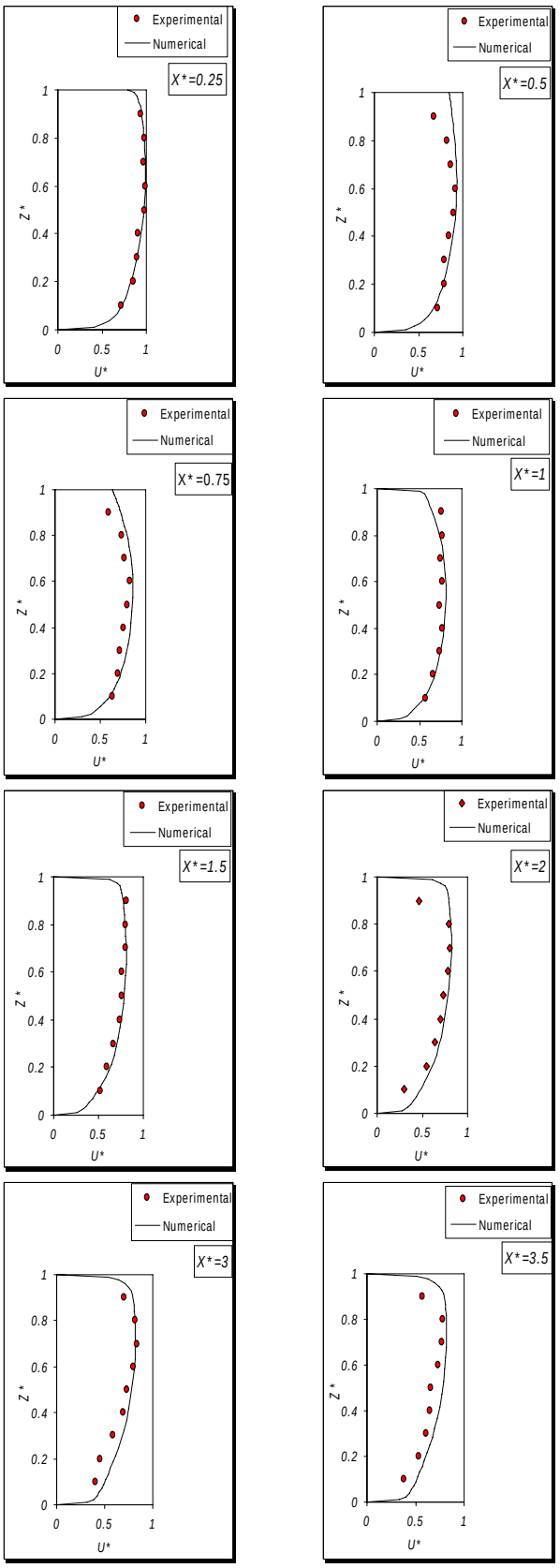

Fig. 4 Velocity profile along main-channel (Continued)

As the flow enters the intake structure, the maximum velocity due to the generating separation zone is moved away from the side-channel inner wall ($X^* = 0$)(Fig.5). Having passed through the intake structure, the remaining flow in the main-channel is developed into downstream main-channel. However, the maximum flow velocity is returned to downstream main-channel inner wall because of the bending effects of the flow lines ($Z^* = 1$).

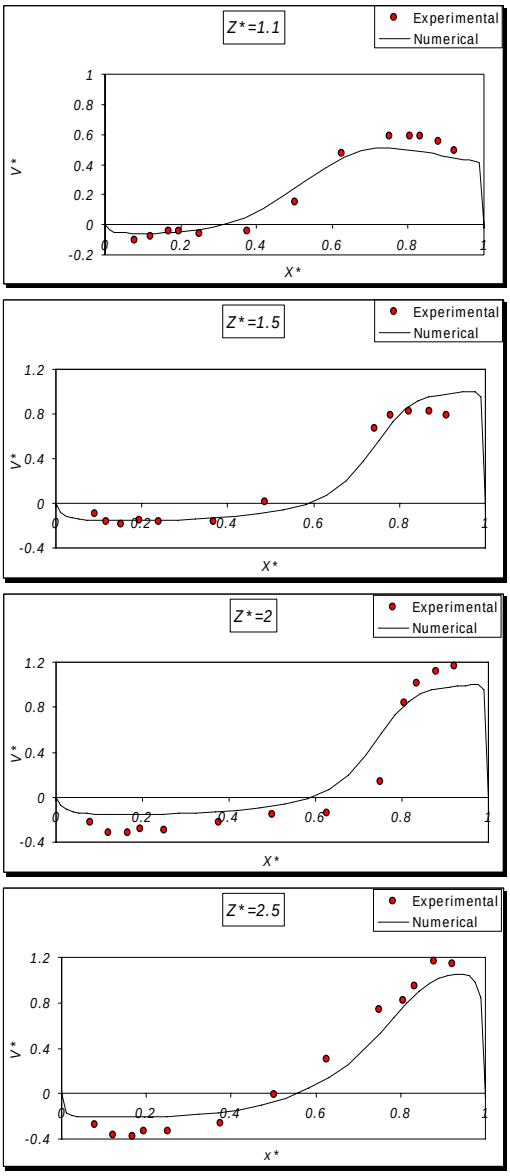

Fig. 5 Velocity profile along side-channel

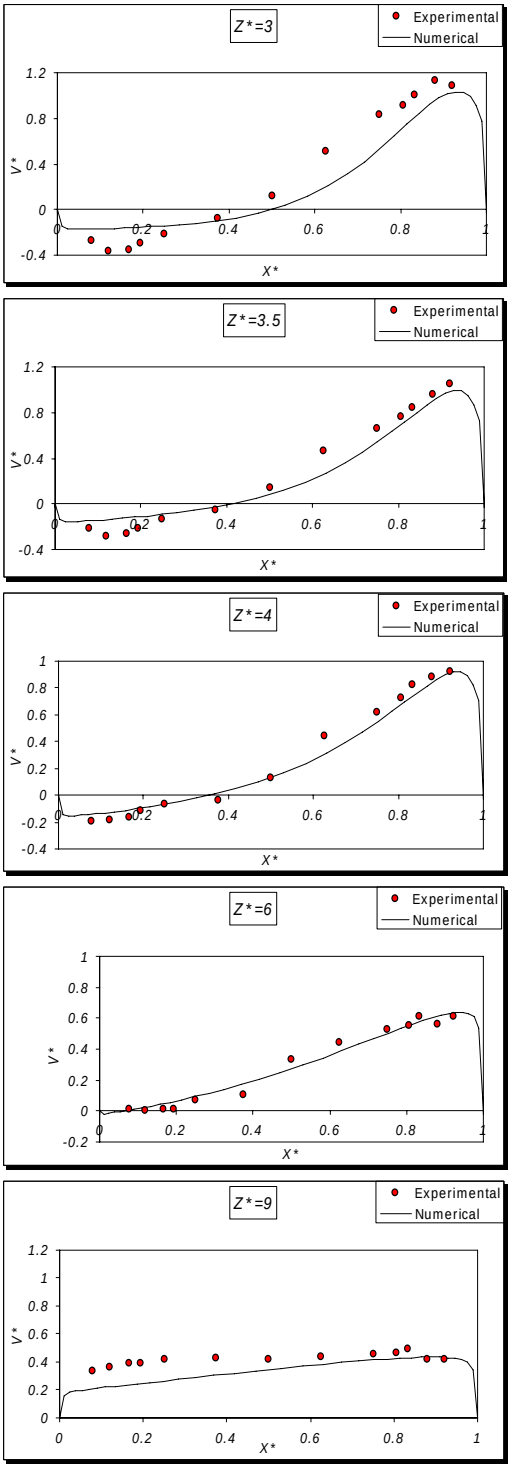

Fig. 5 Velocity profile along side-channel (Continued)

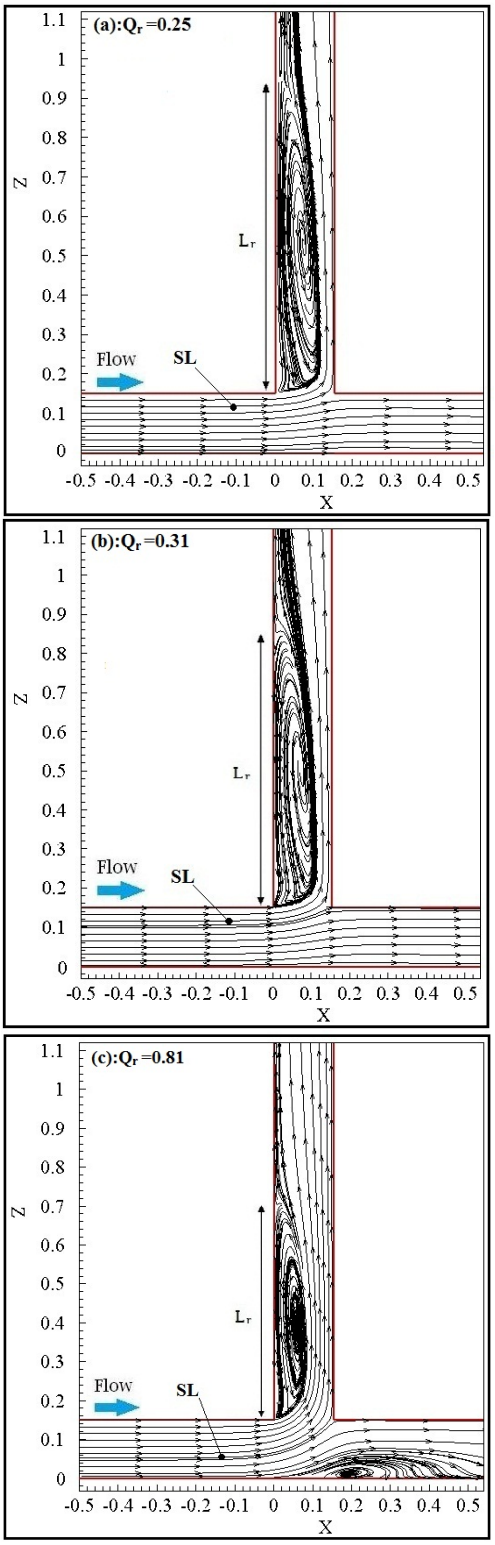

Fig. 6 Streamlines in the plane close to water surface

Comparison of results (Fig.6) shows that by increasing the discharge ratio, the length and width of separation zone in the intake structures are considerably decreased. By contrast the increase in discharge ratio is shown to have a corresponding increase in distance of the flow dividing line from the main-channel inner wall. The dimensionless width of the separation zone has clearly indicated a close proximity between the model outputs and the experimental data (Fig.7) [4].

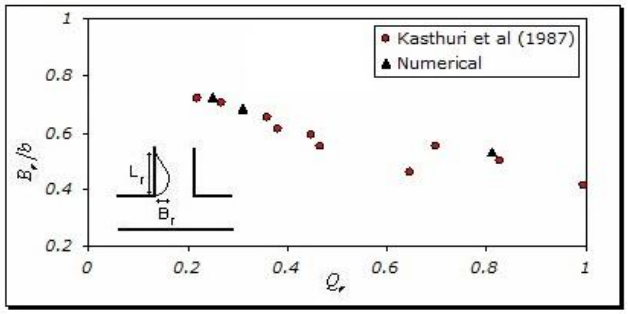

Fig. 7 Dimensionless width of the separation zone

NOTATION

u_i = Velocity components in Cartesian coordinates (u, v, w);

U^* = Ratio of *x* direction velocity to maximum velocity at ($X^* = -4.15$);

W^* = Ratio of *y* direction velocity to maximum velocity at ($X^* = -4.15$);

V^* = Ratio of *z* direction velocity to maximum velocity at ($X^* = -4.15$);

P = Total pressure;

ρ = Water density;

g_i = Gravity acceleration in Cartesian coordinate;

τ_{ij} = Stress tensor;

H_0 = Water depth at main-channel entrance;

Q_1 = Inflow;

Q_2 = Side-channel outflow;

Q_3 = Main-channel outflow;

Q_r = Ratio of side-channel to total discharge;

F_r = Frude number $\left(= U_0 / \sqrt{gH_0}\right)$;

R_e = Reynolds number $\left(= \rho U_0 H_0 / \mu\right)$;

μ = Fluid viscosity;

μ_t = Eddy viscosity;

L_r = Length of separation zone;

B_r = Width of separation zone;

k = Turbulent kinetic energy;

ε = Turbulent dissipation rate;

X^* = Ratio of *x* to channel width;

Y^* = Ratio of *y* to channel width;

Z^* = Ratio of *z* to channel width;

REFERENCES

[1] Barkdoll, B.D. (1998)."Sediment control at lateral diversion". PhD dissertation, Civil and Environmental Engineering, University of Iowa.

[2] Grace, J.L. and Pirest, M.S. (1958)."Division of flow in an open-channel junction". Bulletin No.31, Engineering Experimental Station, Alabama Polytechnic Institute.

[3] Hsu, C.C., Tang, C.J., Lee, W.J., and Shieh, M.Y. (2002)."Subcritical 90^0 equal-width open-channel dividing flow". Journal of Hydraulic Engineering. ASCE, 128(7), 716-720.

[4] Kasthuri, B. and Pundarikanthan, N.V. (1987)."Discussion of separation zone at open-channel junction". Journal of Hydraulic Engineering. ASCE, 113(4), 543-544.

[5] Krishnappa, G. and Seetharamiah, K. (1963)."Anew method of predicting the flow in a 90 branch channels". La Houlle Blanche, No.7.

[6] Law and Reynolds. (1966)."Division of flow in an open-channel". Journal of Hydraulic Engineering. ASCE, 192(2), 207-231.

[7] Ramamurthy, A.S. and Sitish, M.G. (1987)."Internal hydraulics of diffusers with uniform lateral momentum distribution". Journal of Hydraulic Engineering. ASCE, 113(3), 449-463.

[8] Ramamurthy, A.S., QU, J., and VO, D. (2007)."Numerical and experimental study of dividing open-channel flow". Journal of Hydraulic Engineering. ASCE, 113(10), 1135-1144.

[9] Rameshwaran, P., and Shiono, K. (2007)."Quasi two-dimensional model for straight overbank flows through emergent vegetation on floodplains". Journal of Hydraulic Research. 45, 302-315.

[10] Rodi, W. (1979)."Turbulent models and their application in hydraulics-at state-of-the art review".IAHR, Delft, Netherlands.

[11] Sridharan, K. (1966)."Division of flow in open-channels". Thesis, India Institute of science, Banglor, India.

[12] Taylor, E.H. (1944)."Flow characteristics at rectangular open-channel junction". Journal of Hydraulic Engineering. ASCE, 109, 893-912.

[13] Yakhot, V., Orszag, S.A., Thangam, S., Gatski, T.B. & Speziale, C.G. (1992)."Development of turbulence models for shear flows by a double expansion technique". Physics of Fluids, Vol. 4, No. 7, and pp1510-1520.